INTERNATIONAL JOURNAL FOR NUMERICAL METHODS IN FLUIDS
Int. J. Numer. Meth. Fluids 2007; **54**:1313–1325
Published online 23 January 2007 in Wiley InterScience (www.interscience.wiley.com). DOI: 10.1002/fld.1427

On a boundary condition for pressure-driven laminar flow of incompressible fluids

William L. Barth[1,*,†] and Graham F. Carey[2]

[1]*The University of Texas at Austin, ROC 1.405, J.J. Pickle Research Campus, 10100 Burnet Road (R8700), Building 196, Austin, TX 78758-4497, U.S.A.*
[2]*CFDLab, ICES, The University of Texas at Austin, 1 University Station, Mail Code: C0600, Austin, TX 78712, U.S.A.*

SUMMARY

We prove in Theorem 1 a new relationship between the stress, pressure, velocity, and mean curvature for embedded surfaces in incompressible viscous flows. This is then used to define a corresponding modified pressure boundary condition for flow of Newtonian and generalized Newtonian fluids. These results agree with an intuitive notion of the flow physics but apparently have not previously been shown rigorously. We describe some of the implementation issues for inflow and outflow boundaries in this context and give details for a penalty treatment of the associated tangential velocity constraint. This is then implemented and applied in high-resolution 3D benchmark calculations for a representative generalized viscosity model.

Received 31 March 2006; Revised 28 November 2006; Accepted 2 December 2006

KEY WORDS: pressure boundary conditions; incompressible Navier–Stokes; generalized Newtonian fluids; finite-element methods

1. INTRODUCTION

The numerical simulation of Newtonian and generalized Newtonian flows poses a number of challenges. Of particular interest here is the choice of appropriate inflow and outflow boundary conditions. In certain pipe and channel-flow problems involving Newtonian fluids an analytic, fully-developed profile can be determined. Such profiles may then be applicable as remote boundary conditions in numerical simulations. However, analytic solutions are usually not available for generalized Newtonian fluids especially in more complex geometries. Hence, the specification of a known fully developed velocity profile is generally not an option.

*Correspondence to: William L. Barth, The University of Texas at Austin, ROC 1.405, J.J. Pickle Research Campus, 10100 Burnet Road (R8700), Building 196, Austin, TX 78758-4497, U.S.A.
†E-mail: bbarth@tacc.utexas.edu

Special boundary conditions can also be devised for remote far field or exterior flows to approximate remote boundary conditions (e.g. see [1–5]). Of course, traction boundary conditions may be applicable, and there have been several studies in the literature on such forms of outflow boundary conditions. For example, it is common to impose a zero-normal-stress condition at the outflow of the domain when the velocity is not known [6, 7].

To motivate our study here with generalized Newtonian flows, we find it instructive to consider first what conditions might be easily determined or imposed in a laboratory experiment. For instance, a pump, pressurized vessel, or fluid column could be used to bring fluid at a known pressure to the entrance of a pipe or channel test section under investigation (as in wind and water tunnels). The static entry pressure could be measured by a single experiment and the velocity profile could be determined there by detailed local measurement. At the outflow, provided laminar flow conditions persist, one might make similar pressure or velocity measurements. Also, if the geometry of the domain is simple, then one may be able to apply a semi-analytic approach to construct an approximate velocity profile. The momentum equations may be reduced and integrated once to yield a 1D ordinary differential equation (ODE) that can be numerically integrated [8].

For those real-world problems that are fundamentally pressure driven and involve more complex geometries, it is desirable then to impose a pressure drop by means of specified pressures at the inflow and outflow boundaries. However, this is not mathematically justifiable for many common finite element formulations for the incompressible Navier–Stokes equations including mixed-Galerkin and pressure-projection methods as it leads to ill-posed problems and stability concerns [6, 9]. Consequently, our goal here is to examine the role of the pressure more rigorously in this context for Newtonian and generalized Newtonian fluids.

We begin with a brief statement of the governing equations and constitutive relations of interest and in Theorem 1, construct a relation between stress, pressure, velocity, and mean curvature of embedded surfaces. This relation may then be applied to prescribe appropriate pressure inflow or outflow boundary conditions. Computationally, it is convenient to implement the boundary condition using a penalty variational approach. This formulation is described, interpreted, and implemented in a finite element scheme for generalized Newtonian flow simulation. Numerical benchmark examples with a Powell–Eyring viscosity model are conducted for several pipe-flow geometries.

2. PRESSURE RELATION

We consider here the standard primitive-variables statement of the continuity and momentum equations describing incompressible, viscous flow of a generalized Newtonian fluid

$$\rho \frac{\partial \mathbf{u}}{\partial t} + \mathbf{u} \cdot \nabla \mathbf{u} = \nabla \cdot \boldsymbol{\sigma}, \quad (\mathbf{x}, t) \in \Omega \times [0, t_f] \tag{1}$$

$$\nabla \cdot \mathbf{u} = 0 \tag{2}$$

where Ω is the spatial domain, t_f is the final time of interest, $\mathbf{u}$ is the unknown velocity vector, ρ is the density, and $\boldsymbol{\sigma}$ is the stress tensor. The constitutive equation for the fluid stress is given by

$$\boldsymbol{\sigma} = -p\mathbf{I} + 2\mu\mathbf{D}(\mathbf{u}) \tag{3}$$

DOI: 10.1002/fld

where $\mathbf{I}$ is the identity tensor, μ is the (not necessarily constant) viscosity, and $\mathbf{D}(\mathbf{u})$ is the strain rate tensor given by

$$\mathbf{D}(\mathbf{u}) = \tfrac{1}{2}(\nabla\mathbf{u} + (\nabla\mathbf{u})^{\mathrm{T}}) \tag{4}$$

For any velocity-normal surface ($\Gamma_p \subset \partial\Omega$) let us define the normal component of the surface traction force to be

$$(\boldsymbol{\sigma}(\mathbf{x}, t) \cdot \hat{\mathbf{n}}) \cdot \hat{\mathbf{n}} = \sigma_p(\mathbf{x}, t), \quad (\mathbf{x}, t) \in \Gamma_p \times [0, t_{\mathrm{f}}] \tag{5}$$

where $\hat{\mathbf{n}}$ is the outward unit normal to Γ_p.

Theorem 1
For any velocity-normal surface ($\Gamma_p \subset \partial\Omega$) in an incompressible viscous fluid, the normal component of the normal traction is given by

$$\sigma_p(\mathbf{x}, t) = -(p + 2\mu(\mathbf{u})|\mathbf{u}|\kappa) \tag{6}$$

where κ is the mean curvature of Γ_p. Furthermore, in the case where Γ_p is a planar surface, this reduces to the pressure condition

$$p(\mathbf{x}, t) = -\sigma_p(\mathbf{x}, t), \quad (\mathbf{x}, t) \in \Gamma_p \times [0, t_{\mathrm{f}}] \tag{7}$$

Proof
Combining Equations (3) and (4), the constitutive relation becomes

$$\boldsymbol{\sigma} = -\mathbf{I}p + \mu(\mathbf{u})(\nabla\mathbf{u} + (\nabla\mathbf{u})^{\mathrm{T}}) \tag{8}$$

Now, given any unit vector field, $\hat{\mathbf{v}}$, the following identities hold:

$$\begin{aligned}(\boldsymbol{\sigma} \cdot \hat{\mathbf{v}}) \cdot \hat{\mathbf{v}} &= \{[-p\mathbf{I} + \mu(\mathbf{u})(\nabla\mathbf{u} + (\nabla\mathbf{u})^{\mathrm{T}})] \cdot \hat{\mathbf{v}}\} \cdot \hat{\mathbf{v}} \\ &= -(p\mathbf{I}\hat{\mathbf{v}}) \cdot \hat{\mathbf{v}} + \{[\mu(\mathbf{u})(\nabla\mathbf{u} + (\nabla\mathbf{u})^{\mathrm{T}})] \cdot \hat{\mathbf{v}}\} \cdot \hat{\mathbf{v}} \qquad (9) \\ &= -p\hat{\mathbf{v}} \cdot \hat{\mathbf{v}} + (2\mu(\mathbf{u})(\nabla\mathbf{u}) \cdot \hat{\mathbf{v}}) \cdot \hat{\mathbf{v}} \quad \text{since } ((\nabla\mathbf{u}) \cdot \hat{\mathbf{v}}) \cdot \hat{\mathbf{v}} = ((\nabla\mathbf{u})^{\mathrm{T}} \cdot \hat{\mathbf{v}}) \cdot \hat{\mathbf{v}} \\ &= -p + (2\mu(\mathbf{u})(\nabla\mathbf{u}) \cdot \hat{\mathbf{v}}) \cdot \hat{\mathbf{v}} \quad \text{since } |\hat{\mathbf{v}}| = 1 \qquad (10)\end{aligned}$$

For the velocity field, $\mathbf{u} = (u_1, u_2, u_3)$ and co-ordinates $\mathbf{x} = (x_1, x_2, x_3)$, streamlines may be defined by integrating the following equations:

$$\frac{\mathrm{d}x_1}{u_1} = \frac{\mathrm{d}x_2}{u_2} = \frac{\mathrm{d}x_3}{u_3} \tag{11}$$

Next, let us take $\hat{\mathbf{v}}$ to be the unit tangent vector field to these streamlines, then the velocity can may be expressed as

$$\mathbf{u} = |\mathbf{u}|\hat{\mathbf{v}} \tag{12}$$

DOI: 10.1002/fld

Substituting Equation (12) for $\mathbf{u}$ in terms of $\hat{\mathbf{v}}$ into the reduced part of the viscous term and simplifying

$$\begin{aligned}(\boldsymbol{\sigma}\cdot\hat{\mathbf{v}})\cdot\hat{\mathbf{v}} &= -p + 2\mu(\mathbf{u})(\nabla(|\mathbf{u}|\hat{\mathbf{v}})\cdot\hat{\mathbf{v}})\cdot\hat{\mathbf{v}}\\ &= -p + 2\mu(\mathbf{u})\{(\nabla|\mathbf{u}|)\cdot\hat{\mathbf{v}}(\hat{\mathbf{v}}\cdot\hat{\mathbf{v}}) + |\mathbf{u}|[(\nabla\hat{\mathbf{v}})\cdot\hat{\mathbf{v}}]\cdot\hat{\mathbf{v}}\}\\ &= -p + 2\mu(\mathbf{u})\{(\nabla|\mathbf{u}|)\cdot\hat{\mathbf{v}} + |\mathbf{u}|[(\nabla\hat{\mathbf{v}})\cdot\hat{\mathbf{v}}]\cdot\hat{\mathbf{v}}\}\end{aligned}$$

Since

$$\begin{aligned}((\nabla\hat{\mathbf{v}})\cdot\hat{\mathbf{v}})\cdot\hat{\mathbf{v}} &= \tfrac{1}{2}(\nabla|\hat{\mathbf{v}}|^2)\cdot\hat{\mathbf{v}} + (\hat{\mathbf{v}}\times(\nabla\times\hat{\mathbf{v}}))\cdot\hat{\mathbf{v}}\\ &= \nabla 1\cdot\hat{\mathbf{v}} + (\hat{\mathbf{v}}\times(\nabla\times\hat{\mathbf{v}}))\cdot\hat{\mathbf{v}}\\ &= 0\end{aligned}$$

it follows that

$$(\boldsymbol{\sigma}\cdot\hat{\mathbf{v}})\cdot\hat{\mathbf{v}} = -p + 2\mu(\mathbf{u})(\nabla|\mathbf{u}|)\cdot\hat{\mathbf{v}} \tag{13}$$

Next, substituting Equation (12) into the continuity equation, (2), gives

$$0 = \nabla\cdot\mathbf{u} = \nabla\cdot(|\mathbf{u}|\hat{\mathbf{v}}) = (\nabla|\mathbf{u}|)\cdot\hat{\mathbf{v}} + |\mathbf{u}|\nabla\cdot\hat{\mathbf{v}} \tag{14}$$

Using this, (13) becomes

$$(\boldsymbol{\sigma}\cdot\hat{\mathbf{v}})\cdot\hat{\mathbf{v}} = -(p + 2\mu(\mathbf{u})|\mathbf{u}|\nabla\cdot\hat{\mathbf{v}}) \tag{15}$$

Finally, restricting to Γ_p, taking $\hat{\mathbf{v}}$ as $\hat{\mathbf{n}}$, the outward unit normal to Γ_p, and recalling that $\kappa = (\nabla\cdot\hat{\mathbf{v}})|_{\Gamma_p}$ is the mean curvature of Γ_p, implies

$$(\boldsymbol{\sigma}|_{\Gamma_p}\hat{\mathbf{n}})\cdot\hat{\mathbf{n}} = -(p + 2\mu(\mathbf{u})|\mathbf{u}|\kappa) \tag{16}$$

□

This then is the main result linking stress, pressure, velocity, and mean curvature on any velocity-normal embedded surface. In the special case where velocity-normal surface Γ_p is planar, then $\kappa = 0$, and we obtain a simplified result involving only the pressure. This is the case in the planar outflow boundary considered in subsequent numerical experiments. (Note: if Γ_p is an inflow boundary, then the curvature term would appear with a negative sign above.)

A few items from the above analysis merit further comment. First, Equation (10) above is a general statement applicable anywhere in the flow for any unit vector field giving an identity between the normal component of the normal traction, the pressure, and the velocity gradient. Second, Equation (15) is similarly valid anywhere in the flow, but it applies only to those vectors tangent to the streamlines. Finally, Equation (16) is applicable on any embedded surface in the flow field (interior or on the inflow/outflow boundaries) to which the velocity is an outward normal. This final equation relates the normal component of the normal traction, the pressure, the velocity magnitude, and the surface mean curvature. If the associated surface is planar and an inflow or outflow boundary then we have the simplified (planar) pressure boundary condition in Equation (7).

DOI: 10.1002/fld

We now summarize the initial and boundary conditions completing the statement of the flow problem. For convenience we assume an initially quiescent flow (though the proposed technique does not require this condition as long as the initial condition is divergence-free)

$$\mathbf{u}(\mathbf{x}, 0) = \mathbf{0}, \quad \mathbf{x} \in \Omega \tag{17}$$

On the solid walls of the domain Ω we specify the usual no-slip and no-penetration conditions

$$\mathbf{u} = \mathbf{0}, \quad (\mathbf{x}, t) \in \Gamma_D \times [0, t_f] \tag{18}$$

where $\Gamma_D \subset \partial\Omega$.

At the inflow and outflow boundaries ($\Gamma_p \subset \partial\Omega$) we set

$$(\boldsymbol{\sigma}(\mathbf{x}, t) \cdot \hat{\mathbf{n}}) \cdot \hat{\mathbf{n}} = \sigma_p(\mathbf{x}, t), \quad (\mathbf{x}, t) \in \Gamma_p \times [0, t_f] \tag{19}$$

$$\mathbf{u} \cdot \hat{\boldsymbol{\tau}}_1 = 0 \tag{20}$$

$$\mathbf{u} \cdot \hat{\boldsymbol{\tau}}_2 = 0 \tag{21}$$

where $\hat{\mathbf{n}}$ is the outward unit normal, $\sigma_p(\mathbf{x}, t)$ is the pressure expression and $\hat{\boldsymbol{\tau}}_1$ and $\hat{\boldsymbol{\tau}}_2$ are unit tangent vectors to Γ_p. The first condition specifies the normal component of the surface traction force, and the latter two imply there is no tangential flow at these boundaries; that is, flow is normal to the inflow and outflow boundaries. This corresponds exactly to the conditions of Theorem 1 and, therefore, acts as a pressure boundary condition. As an example, in the pipe flow cases computed later, if the surface Γ_p is perpendicular to the pipe walls, then Equations (20) and (21) correspond to requiring that the flow be parallel to the pipe walls at this boundary, otherwise they simply require the flow to be normal to Γ_p.

3. PENALTY VARIATIONAL FORMULATION

A penalty formulation for a Galerkin finite element scheme is used in subsequent numerical experiments concerning the boundary conditions discussed above. The associated weak formulation of the governing equations is derived by multiplying Equations (1) and (2) by appropriate test functions, integrating over the domain Ω, applying integration by parts to the viscous stress term and introducing the constitutive relations to obtain:

Find $(\mathbf{u}, p) \in \mathbf{V} \times Q$ satisfying the essential boundary conditions, (19), and such that

$$\int_\Omega \rho \left(\frac{\partial \mathbf{u}}{\partial t} + \mathbf{u} \cdot \nabla \mathbf{u} \right) \cdot \mathbf{v} \, \mathrm{d}x$$

$$= \int_\Omega p(\nabla \cdot \mathbf{v}) - 2\mu \mathbf{D}(\mathbf{u}) : \nabla \mathbf{v} \, \mathrm{d}x + \int_{\Gamma_p} (\boldsymbol{\sigma} \cdot \hat{\mathbf{n}}) \cdot \mathbf{v} \, \mathrm{d}s \tag{22}$$

$$- \int_\Omega q(\nabla \cdot \mathbf{u}) \, \mathrm{d}x = 0 \tag{23}$$

for all admissible test functions $(\mathbf{v}, q) \in \mathbf{V} \times Q$.

DOI: 10.1002/fld

Note that we have retained the normal traction in the boundary term arising from integration by parts in the basic formulation.

The normal-traction boundary condition is applied by rewriting the boundary integral in Equation (22) as

$$\int_{\Gamma_p} (\boldsymbol{\sigma} \cdot \hat{\mathbf{n}}) \cdot \mathbf{v} \, \mathrm{d}s = \int_{\Gamma_p} (\boldsymbol{\sigma} \cdot \hat{\mathbf{n}}) \cdot (v_{\hat{\mathbf{n}}} \hat{\mathbf{n}} + v_{\hat{\tau}_1} \hat{\boldsymbol{\tau}}_1 + v_{\hat{\tau}_2} \hat{\boldsymbol{\tau}}_2) \, \mathrm{d}s \tag{24}$$

and substituting Equations (19) and (24) into Equation (22) with $v_{\tau_1} = v_{\tau_2} = 0$, since the tangential velocity components are zero on Γ_p, to get

$$\int_\Omega \rho \left(\frac{\partial \mathbf{u}}{\partial t} + \mathbf{u} \cdot \nabla \mathbf{u} \right) \cdot \mathbf{v} \, \mathrm{d}x = \int_\Omega p(\nabla \cdot \mathbf{v}) - 2\mu \mathbf{D}(\mathbf{u}) : \nabla \mathbf{v} \, \mathrm{d}x + \int_{\Gamma_p} \sigma_p v_{\hat{\mathbf{n}}} \, \mathrm{d}s \tag{25}$$

The conditions of no flow tangential to Γ_p (Equations (20) and (21)) or, equivalently, the condition that the flow be entirely normal to it, may be easily implemented as essential boundary conditions directly in the resulting finite element matrix problem when the surface tangents are axis aligned. (e.g. $\mathbf{u} \cdot \hat{\boldsymbol{\tau}}_1 = 0$ would be equivalent to $u_1 = 0$ when $\hat{\boldsymbol{\tau}}_1$ is aligned with the x_1-direction). However, boundary penalty methods are often introduced in finite element software to simplify the treatment of essential conditions in more general situations. In the boundary penalty integral, the tangents or normals are evaluated at the Gauss integration points interior to element boundary edges or faces. This avoids ambiguities due to edge vertex discontinuities in normal and tangential vector directions. It also simplifies the software implementation by using the same integration facilities already employed for constructing the underlying finite element system.

The tangential velocity vector can be determined by subtracting the resolved velocity vector in the normal direction. That is, for the tangential part of the velocity vector we then have: $[\mathbf{u} - (\mathbf{u} \cdot \hat{\mathbf{n}})\hat{\mathbf{n}}]$. In the present work, the condition that the components of the velocity tangent to Γ_p are zero is enforced using a penalty method by adding the first variation of the following least-squares penalty functional to Equation (25):

$$I(\mathbf{u}) = \frac{1}{2\varepsilon} \int_{\Gamma_p} [\mathbf{u} - (\mathbf{u} \cdot \hat{\mathbf{n}})\hat{\mathbf{n}}] \cdot [\mathbf{u} - (\mathbf{u} \cdot \hat{\mathbf{n}})\hat{\mathbf{n}}] \, \mathrm{d}s \tag{26}$$

where $0 < \varepsilon \ll 1$ is the penalty parameter. Taking the first variation, the contribution from the penalty functional is

$$\begin{aligned} I'(\mathbf{u})(\mathbf{v}) &= \frac{1}{\varepsilon} \int_{\Gamma_p} [\mathbf{u} - (\mathbf{u} \cdot \hat{\mathbf{n}})\hat{\mathbf{n}}] \cdot [\mathbf{v} - (\mathbf{v} \cdot \hat{\mathbf{n}})\hat{\mathbf{n}}] \, \mathrm{d}s \\ &= \frac{1}{\varepsilon} \int_{\Gamma_p} \{\mathbf{u} \cdot \mathbf{v} - [(\mathbf{u} \cdot \hat{\mathbf{n}})\hat{\mathbf{n}}] \cdot \mathbf{v} - \mathbf{u} \cdot [(\mathbf{v} \cdot \hat{\mathbf{n}})\hat{\mathbf{n}}] + [(\mathbf{u} \cdot \hat{\mathbf{n}})\hat{\mathbf{n}}] \cdot [(\mathbf{v} \cdot \hat{\mathbf{n}})\hat{\mathbf{n}}]\} \, \mathrm{d}s \\ &= \frac{1}{\varepsilon} \int_{\Gamma_p} \mathbf{u} \cdot \mathbf{v} + (\mathbf{u} \cdot \hat{\mathbf{n}})(\mathbf{v} \cdot \hat{\mathbf{n}}) - 2(\mathbf{u} \cdot \hat{\mathbf{n}})(\mathbf{v} \cdot \hat{\mathbf{n}}) \, \mathrm{d}s \\ &= \frac{1}{\varepsilon} \int_{\Gamma_p} \mathbf{u} \cdot \mathbf{v} - (\mathbf{u} \cdot \hat{\mathbf{n}})(\mathbf{v} \cdot \hat{\mathbf{n}}) \, \mathrm{d}s \end{aligned} \tag{27}$$

DOI: 10.1002/fld

Adding this penalty contribution to the previous variational functional statement, we have the penalized problem:

Find $(\mathbf{u}, p) \in \mathbf{V} \times Q$ satisfying the essential boundary conditions, Equation (19), and such that

$$\int_\Omega \rho \left(\frac{\partial \mathbf{u}}{\partial t} + \mathbf{u} \cdot \nabla \mathbf{u} \right) \cdot \mathbf{v} \, \mathrm{d}x = \int_\Omega p(\nabla \cdot \mathbf{v}) - 2\mu D(\mathbf{u}) : \nabla \mathbf{v} \, \mathrm{d}x + \int_{\Gamma_p} \sigma_p v_{\hat{\mathbf{n}}} \, \mathrm{d}s + \frac{1}{\varepsilon} \int_{\Gamma_p} \mathbf{u} \cdot \mathbf{v} - (\mathbf{u} \cdot \hat{\mathbf{n}})(\mathbf{v} \cdot \hat{\mathbf{n}}) \, \mathrm{d}s \tag{28}$$

$$- \int_\Omega q(\nabla \cdot \mathbf{u}) \, \mathrm{d}x = 0 \tag{29}$$

for all admissible test functions $(\mathbf{v}, q) \in \mathbf{V} \times Q$.

Alternatively, one can view the addition of the penalty as a mixed boundary condition involving the tangential components of the velocity and the tangential components of the normal traction. The normal traction is given by

$$\boldsymbol{\sigma} \cdot \hat{\mathbf{n}} = -p\hat{\mathbf{n}} + \mu(\mathbf{u})(\nabla \mathbf{u} + (\nabla \mathbf{u})^{\mathrm{T}}) \cdot \hat{\mathbf{n}}$$

Expanding the velocity gradient terms in surface co-ordinates and simplifying gives

$$\boldsymbol{\sigma} \cdot \hat{\mathbf{n}} = -p\hat{\mathbf{n}} + \mu(\mathbf{u}) \left[2\frac{\partial u_{\hat{\mathbf{n}}}}{\partial \hat{\mathbf{n}}} + \left(\frac{\partial u_{\hat{\boldsymbol{\tau}}_1}}{\partial \hat{\mathbf{n}}} + \frac{\partial u_{\hat{\mathbf{n}}}}{\partial \hat{\boldsymbol{\tau}}_1} \right) \hat{\boldsymbol{\tau}}_1 + \left(\frac{\partial u_{\hat{\boldsymbol{\tau}}_2}}{\partial \hat{\mathbf{n}}} + \frac{\partial u_{\hat{\mathbf{n}}}}{\partial \hat{\boldsymbol{\tau}}_2} \right) \hat{\boldsymbol{\tau}}_2 \right] \tag{30}$$

(Note that this expansion assumes a Cartesian normal-tangential co-ordinate system, and that additional terms from the Christoffel symbols would appear in curvilinear co-ordinates.)

As was done in Equation (24), the normal component of the normal traction in Equation (30) is prescribed as σ_p in the boundary conditions. However, now we can see that setting the tangential components of the test functions to zero in Equation (24) and then adding the penalty for the tangential components of the velocity is equivalent to setting

$$\frac{1}{\varepsilon} u_1 = -\mu(\mathbf{u}) \left(\frac{\partial u_{\hat{\boldsymbol{\tau}}_1}}{\partial \hat{\mathbf{n}}} + \frac{\partial u_{\hat{\mathbf{n}}}}{\partial \hat{\boldsymbol{\tau}}_1} \right) \tag{31}$$

$$\frac{1}{\varepsilon} u_2 = -\mu(\mathbf{u}) \left(\frac{\partial u_{\hat{\boldsymbol{\tau}}_2}}{\partial \hat{\mathbf{n}}} + \frac{\partial u_{\hat{\mathbf{n}}}}{\partial \hat{\boldsymbol{\tau}}_2} \right) \tag{32}$$

That is, the penalty term plus the remaining part of the viscous stress form a natural, mixed boundary condition as one might anticipate. Multiplying these relations throughout by ε makes it clear that the tangential velocities will be $O(\varepsilon \|\mathbf{D}(\mathbf{u})\|)$.

In the examples that follow, Equations (28) and (29) are discretized using the familiar consistent C^0 piecewise quadratic velocities and piecewise linear pressure base pair. The resulting semidiscrete ODE system is integrated in time using a second-order Adams–Bashforth/trapezoidal rule predictor–corrector method, and the resulting nonlinear system in each timestep is iteratively solved to a specified tolerance using Newton's method [10–13].

DOI: 10.1002/fld

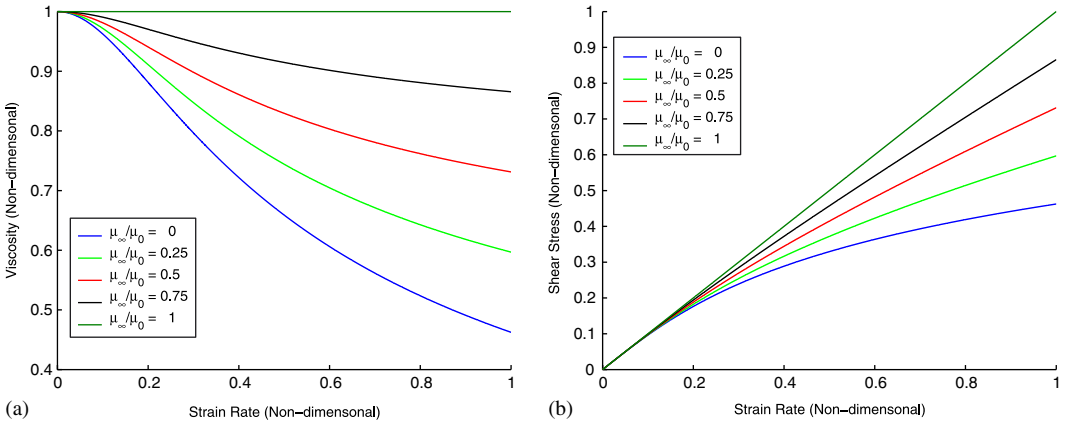

Figure 1. Powell–Eyring model: (a) viscosity; and (b) shear stress.

4. VISCOSITY MODEL

As a representative test fluid, we consider the Powell–Eyring apparent viscosity model. This model is based on Eyring reaction-rate theory giving it a strong thermodynamic underpinning [14–17]. The theory treats viscous diffusion as a 'rate process' described by a sum of exponential decay terms at the molecular level leading to an expansion of the viscosity in terms of inverse hyperbolic sine functions of the strain rate. Keeping the first two terms in such an expansion leads to the 3-parameter Powell–Eyring model:

$$\mu(s) = \mu_\infty + (\mu_0 - \mu_\infty)\,\frac{\sinh^{-1}(\lambda s)}{\lambda s} \tag{33}$$

where, for strain rate s, μ_0 is the limiting viscosity at zero strain rate, μ_∞ is the limiting viscosity as $s \to \infty$, and λ is a characteristic time. The strain rate is given by

$$s(\mathbf{u}) = \sqrt{2\mathbf{D}(\mathbf{u}) : \mathbf{D}(\mathbf{u})} \tag{34}$$

Dimensionless viscosity, $\mu(s)/\mu_0$, and shear stress magnitude, $s\mu(s)/s_0\mu_0$, are plotted in Figures 1(a) and (b) *versus* strain rate, s/s_0 for $\lambda = 100$ and five linearly spaced values of μ_∞/μ_0 in [0, 1]. Note that the Newtonian fluid is the special case where $\mu_0 = \mu_\infty$.

5. EXAMPLE SIMULATIONS

Now that a viable pressure boundary condition has been established, some example situations for pressure-driven flow in cylindrical pipes are simulated to test the formulation. As a first verification test, velocity profiles are computed from time-dependent solutions to steady state of pressure-driven flow in a straight, cylindrical pipe with a circular cross-section, $L/D = 5$, for Reynolds numbers of 1, 10, and 100, and viscosity ratios of 1, 0.1, and 0.01. Since there is no velocity scale in the problem statement, we take $\rho U^2 = \Delta\sigma$ in the traditional definition of the Reynolds number to

DOI: 10.1002/fld

arrive at a 'pressure' Reynolds number given by

$$Re = \frac{\rho U D}{\mu_0} = \frac{D\sqrt{\Delta\sigma\rho}}{\mu_0} \tag{35}$$

where D is the pipe diameter and $\Delta\sigma = |\sigma_{\text{in}} - \sigma_{\text{out}}|$, where σ_{in} and σ_{out} are the specified normal components of the normal traction at the inflow and outflow boundaries, respectively. This choice leads to a non-dimensional form of the viscosity model given by

$$\mu(s) = \frac{\mu_\infty}{\mu_0} + \left(1 - \frac{\mu_\infty}{\mu_0}\right) \frac{\sinh^{-1}(\lambda^* s)}{\lambda^* s} \tag{36}$$

$$\lambda^* = \frac{\lambda\sqrt{\dfrac{\delta\sigma}{\rho}}}{D} \tag{37}$$

This non-dimensionalization leads to a scheme which is valid for both Newtonian and non-Newtonian cases is valid for all values of the infinite-strain-rate viscosity, μ_∞. However, Equation (36) shows that the non-dimensional viscosity model's characteristic time depends on the real pressure-drop, and so care should be taken when analysing results where the Reynolds number and viscosity ratio are varied and the characteristic time held fixed.

5.1. Straight pipes

Figure 2 shows a representative all-hexahedral mesh for the straight pipe geometry described above, along with a schematic of the boundary conditions. The standard conditions of no-slip with

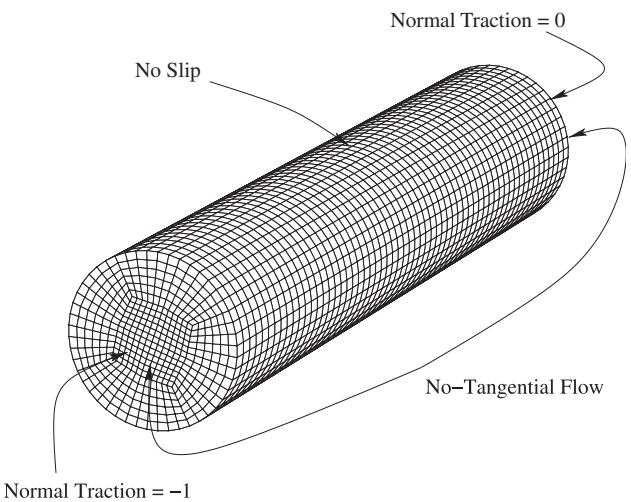

Figure 2. Cylindrical mesh and boundary conditions.

DOI: 10.1002/fld

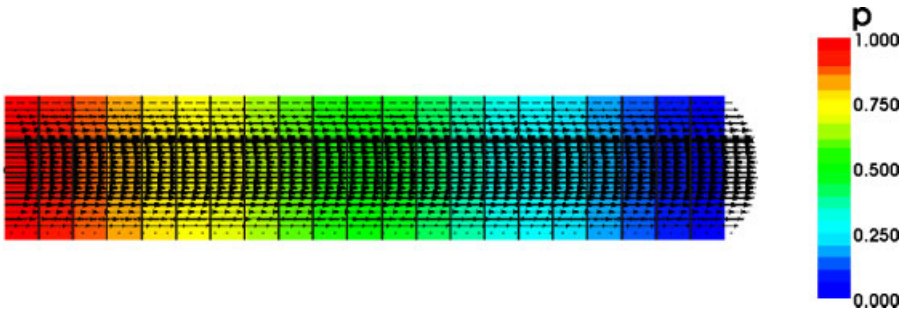

Figure 3. Velocity vectors and pressure contours, $Re = 10$, $\mu_\infty/\mu_0 = 0.1$.

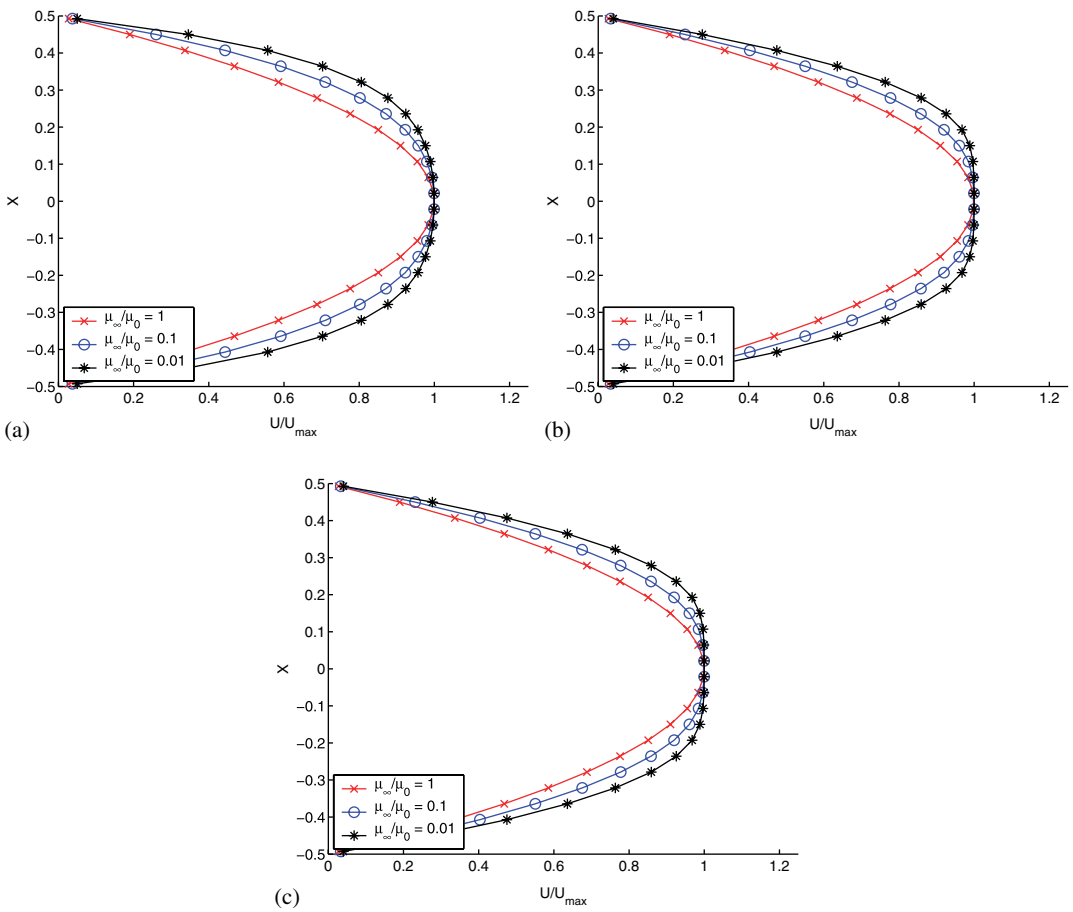

Figure 4. Velocity profiles for Powell–Eyring flow in a cylindrical pipe: (a) $Re = 1$; (b) $Re = 10$; and (c) $Re = 100$.

DOI: 10.1002/fld

no penetration apply at the wall of the cylinder. The inflow and outflow boundary velocity vectors are constrained to be normal to these surfaces in this test (zero tangential velocity components). At the inflow boundary the normal component of the normal traction $\sigma_{\text{in}} = (\boldsymbol{\sigma} \cdot \hat{\mathbf{n}}) \cdot \hat{\mathbf{n}} = -1$ and at the outflow $\sigma_{\text{out}} = 0$ corresponding to a unit non-dimensional pressure drop.

In the following numerical results, the mesh consists of 3240 elements generated by CUBIT [18] partitioned by dividing the domain into eight equal pieces along the length of the cylinder for computation on eight processors. The underlying linear subsystems for the Newton scheme were solved with ILU(0) preconditioned BCGStab to a relative tolerance of 10^{-16} with a maximum of 2000 iterations at each nonlinear step (not required in any of these cases).

Pressure contours and velocity vectors on a mid-pipe cross-section for flow at $Re = 10$ and $\mu_\infty/\mu_0 = 0.1$ are plotted in Figure 3. This demonstrates that the pressure boundary condition is correctly enforced and that the flow is normal to both the inflow and outflow surfaces. Figures 4(a)–(c) show velocity profiles on a longitudinal mid-pipe cross-section halfway downstream from the inflow boundary. As the flow is fully developed and steady, these profiles are identical at all cross-sections in the streamwise direction. Due to the choice of μ_0 as the scaling parameter in the non-dimensionalization, we find that the maximum magnitude of the velocity grows as the viscosity ratio shrinks. However, since we are interested in comparing the shapes of the velocity profiles, we may simply scale these profiles by their respective maximum values to facilitate our comparison as is done in these figures.

These figures illustrate the expected 'plug-flow' behaviour usually associated with shear-thinning fluids as well as the parabolic profile expected in the Newtonian case. At $Re = 1$ the plug-flow profile for the non-Newtonian cases is less blunt and more rounded than those found at higher Reynolds numbers. As is well known, there is no dependence on the Reynolds number for the resulting velocity profile in laminar, fully developed, Newtonian Poiseuille flows. However, for the non-Newtonian case and the non-dimensionalization used in this work, there is an apparent effect of increasing Reynolds number due to the variation of the viscosity. An analysis confirms that, in this scaling, fixing λ^* and varying Re does not correspond to a fixed fluid. To avoid this problem, future numerical experiments might be done with

$$\lambda^* = \frac{\mu_0 \lambda}{D^2 \rho} Re \tag{38}$$

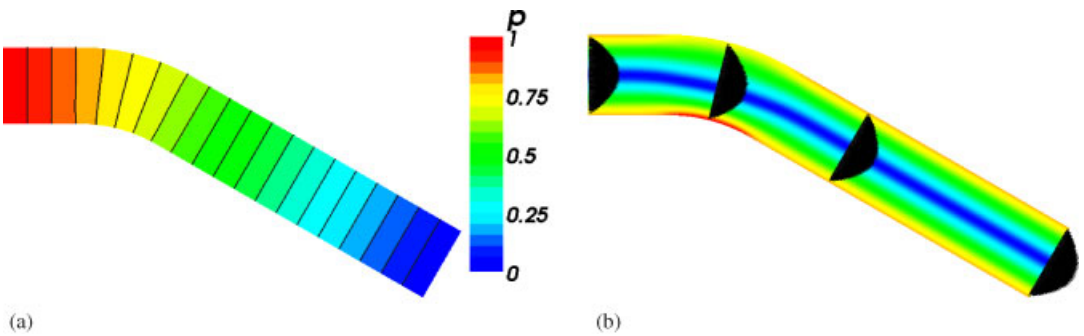

Figure 5. 30° bend, $Re = 10$, $\mu_\infty/\mu_0 = 1$: (a) pressure contours; and (b) velocity vectors and shear stress contours.

DOI: 10.1002/fld

that is, one could introduce a new non-dimensional parameter $\mu_0\lambda/D^2\rho$ which embodies all the material properties. Keeping this fixed as Re varies would result in a non-dimensionalization scheme where the fluid was fixed as the parameters were varied.

5.2. *Bent pipes*

In order to demonstrate the action of the penalty term in the boundary conditions and to give an example where convective effects are important, we also considered pipes with 30, 90, and 120° circular bends. Plotted in Figures 5–7 are pressure contours, section velocity vectors, and contours

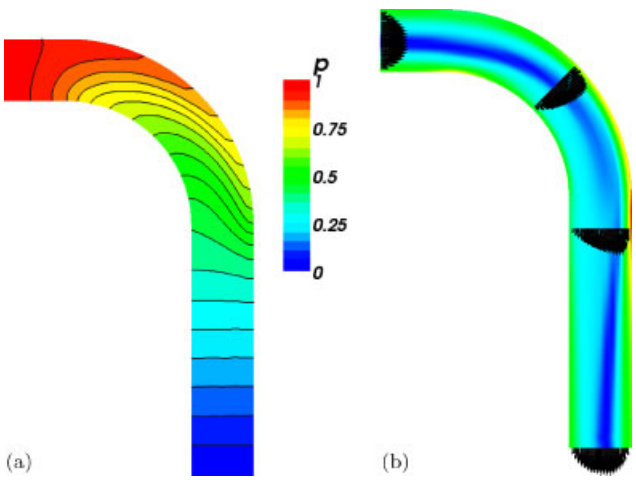

Figure 6. 90° bend, $Re = 40$, $\mu_\infty/\mu_0 = 0.1$: (a) pressure contours; and (b) velocity vectors and shear stress contours.

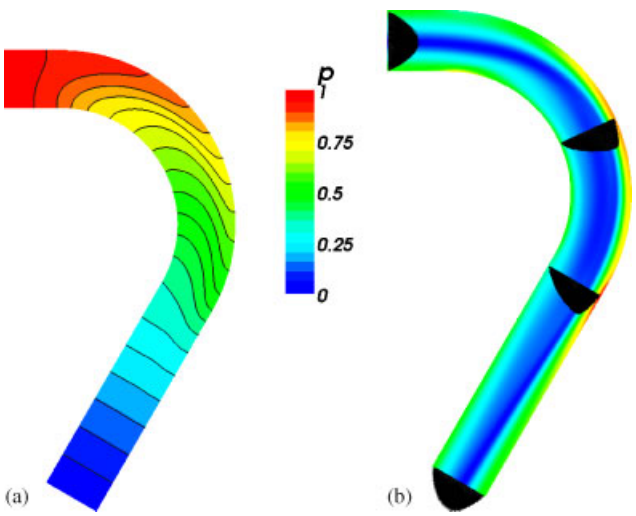

Figure 7. 120° bend, $Re = 200$, $\mu_\infty/\mu_0 = 1$: (a) pressure contours; and (b) velocity vectors and shear stress contours.

DOI: 10.1002/fld

of the magnitude of the shear stress for the 30, 90, and 120° cases, respectively. These figures show clearly that the pressure is constant on the inflow and outflow surfaces, and that the velocity is indeed normal to the inflow and outflow surfaces as expected.

6. CONCLUSIONS

We have established a relationship between the stress, pressure, velocity, and mean curvature on embedded surfaces in incompressible flows where the velocity is normal to the surface. The application of this relation on the inflow or outflow boundary leads to an associated boundary condition. A penalty variational implementation is constructed and interpreted and then used in a finite element scheme. In supporting numerical verification studies for Poiseuille flow in straight 3D pipes, we recover the expected fully developed velocity profiles for Newtonian and generalized Newtonian Powell–Eyring fluids. (The latter are representative of a class of apparent viscosity models.) Other numerical studies on flow in bent pipes illustrate the behaviour of the boundary condition and its penalty implementation. Our intent is to use this boundary condition in future studies of blood flow in arterial branches and other flow simulations.

REFERENCES

1. Carey GF. *Computational Grids*: *Generation*, *Adaptation*, *and Solution Strategies*. Taylor & Francis: London, 1997.
2. Seager M, Carey GF. Adaptive domain extension and adaptive grids for unbounded spherically elliptic PDEs. *SIAM Journal on Scientific and Statistical Computing* 1990; **11**(1):92–111.
3. Heywood JG, Rannacher R, Turek S. Artificial boundary conditions and flux and pressure conditions for the incompressible Navier–Stokes equations. *IJNMF* 1996; **22**(5):325–352.
4. Bose A, Carey GF. Least-squares $p-r$ finite element methods for incompressible non-Newtonian flows. *CMAME* 2000; **180**:431–458.
5. Griffiths DF. The 'no boundary condition' outflow boundary condition. *IJNMF* 1997; **24**:393–411.
6. Gresho PM, Sani RL. *Incompressible Flow and the Finite Element Method*. Wiley: New York, 1998.
7. Sani RL, Gresho PM. Résumé and remarks on the open boundary condition minsymposium. *IJNMF* 1994; **18**:983–1008.
8. Byron Bird B, Armstrong RC, Hassager O. *Dynamics of Polymeric Liquids* (2nd edn), vol. 1. Wiley: New York, 1977.
9. Gresho PM, Sani RL. On pressure boundary conditions for the incompressible Navier–Stokes equations. *International Journal for Numerical Methods in Fluids* 1987; **7**:1111–1145.
10. Carey GF, McLay R, Barth W, Swift S, Kirk B. Distributed parallel simulation of surface tension driven viscous flow and transport processes. *Computational Fluid Dynamics*: *Proceedings of the Fourth UNAM Supercomputing Conference*, UNAM, June 2000; 143–155.
11. Barth W, Carey GF, Kirk B, McLay R. Parallel distributed solution of viscous flow with heat transfer on workstation clusters. *High Performance Computing '00 Proceedings*, Washington, DC, April 2000.
12. Barth W, Carey GF, Chow S, Kirk B. Finite element modeling of generalised newtonian flows. *Proceedings of the 14th Australasian Fluids Conference*, Adelaide, December 2001.
13. Barth WL. Simulation of non-Newtonian fluids on workstation clusters. *Ph.D. Thesis*, The University of Texas at Austin, May 2004.
14. Eyring H. Viscosity, plasticity, and diffusion as examples of absolute reaction rates. *Journal of Chemical Physics* 1936; **4**:283–291.
15. Ree T, Eyring H. Theory of non-Newtonian flow. I. Solid plastic system. *Journal of Applied Physics* 1955; **26**(7):793–800.
16. Ree T, Eyring H. Theory of non-Newtonian flow. II. Solution system of high polymers. *Journal of Applied Physics* 1955; **26**(7):800–809.
17. Ree FH, Ree T, Eyring H. Relaxation theory of transport problems in condensed systems. *Industrial Engineering and Chemistry* 1958; **50**(7):1036–1040.
18. Cubit mesh generation toolkit. http://cubit.sandia.gov/

DOI: 10.1002/fld